# Altered photoemission satellites at $CaF_2$- and $SrF_2$-on-Si(111) interfaces

Eli Rotenberg*
*Department of Physics, University of Oregon, Eugene, Oregon 97403*

J. D. Denlinger*
*Department of Physics, University of Wisconsin, Milwaukee, Wisconsin 53211*

Marjorie A. Olmstead
*Department of Physics, P.O. Box 351560, University of Washington, Seattle, Washington 98195-1560*
(Received 29 June 1995)

Bulk and interface photoemission satellite excitations, measured with x-ray photoelectron spectroscopy and x-ray photoelectron diffraction, are compared for thick, thin, and monolayer films of $CaF_2$ and $SrF_2$ on Si(111). Intrinsic satellites are observed for excitation of atoms in the first monolayer, both uncovered and at the buried interface, that differ from those associated with bulk atoms. For F $1s$ excitation, the bulk and interface satellites differ only in width and amplitude; for the cation core excitations (Ca $2p$, Sr $3p$, and Sr $3d$), the observed excitation energies and intensities differ both from the equivalent bulk satellites and among the various core hole states. The results yield new information on the nature of the interface bonding, as well as on the origin of both bulk and interface satellites. Several models are considered, including differential screening, dielectric losses, crystal-field and multiplet effects, and interface excitation. The most likely explanation for the new cation satellites at the $CaF_2$/Si(111) [$SrF_2$/Si(111)] interface is localized excitation of the interface bond, where the interface band gap is controlled by the collapse of the Ca $3d$ (Sr $4d$) level in the presence of the Ca (Sr) core hole.

## I. INTRODUCTION

In x-ray photoelectron spectroscopy (XPS), inelastic scattering of the outgoing photoelectron can distort the observed line shapes away from simple Lorentzian functions. The main XPS emission lines are often accompanied by satellite peaks, which are caused by discrete energy losses of the photoelectron as it scatters within the solid. These scattering events can be divided into two categories: intrinsic and extrinsic processes, defined by whether or not the scattering is in the immediate vicinity of the core hole created by the photoelectron excitation.

In XPS of thin films, or for surface-sensitive experiments, the location of the emitting atom (e.g., its proximity to a surface or interface) can lead to energy shifts of the core-level photoemission peaks. These shifts may arise both from the altered chemical state of the atom and from local field effects caused by termination of the solid film. The elastic scattering of electrons emitted from these different atomic sites has yielded important information on the local geometric structure and morphology of an epitaxial film,[1,2] and is especially powerful when these different sites may be distinguished by the energy of the emitted electrons.[3,4] Much less attention, however, has been paid to the altered inelastic scattering associated with different structural sites. Since inelastic scattering peaks are present simultaneously with core-level shifted peaks, an understanding of the loss features can be essential for quantitative interpretation of core-level shifted peaks. In addition, observations of different satellite features from geometrically distinguishable atoms (e.g., at the interface vs within the bulk) within the same material highlight the different electronic structures near each atom. Distinct insulator surface satellites have been observed, for example, at MnO surfaces,[5] but altered satellites at buried interfaces have not previously been reported.

In this paper, we report observations of distinct interface and bulk photoemission satellite structures in thin films of $CaF_2$ and $SrF_2$ on Si(111). The atomic structure of the first layer has been previously established to consist of a nonstoichiometric Si-Ca-F (Refs. 6–8) or Si-Sr-F (Ref. 9) layer, with an interface bond derived from silicon and cation orbitals.[10,11] Subsequent deposition consists of F-Ca-F or F-Sr-F triple layers (TL's), with each ion in a bulklike environment.[3,4,12] Using x-ray photoelectron diffraction (XPD) to confirm the assignments of satellite peaks to bulk or interface atoms, we find that electrons emitted from Ca and Sr atoms bonded to Si exhibit satellite peaks that differ from those characteristic of bulk Ca and Sr emission. For excitation of F atoms adjacent to the interface, we observe intrinsic satellite peaks at similar energies to those for bulk F emission, although the peaks are not as sharp. We discuss the intrinsic nature of these peaks, and show that the new interface cation satellite is consistent with a simple charge-transfer model.

Intrinsic satellites in cation photoemission from transition-metal insulators may arise from a number of different interactions. The principal models proposed in the literature for ions in the $3d^0$ configuration include (i) differential screening of the core hole due to transfer of a ligand electron into a $3d$-like (well-screened main line) or $4s$-like (poorly screened satellite) final state,[13] (ii) band-gap excitations[14] or their associated anion- (or ligand-)based excitons,[15] and (iii) rehybridization of the ligand states with the cation $3d$ levels in the presence of the core hole, leading

 

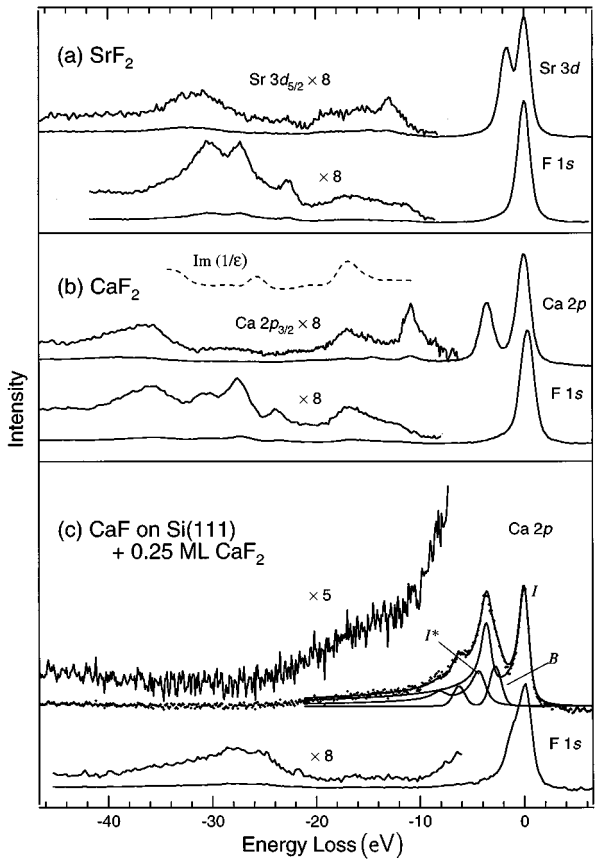


FIG. 1. Bulk and interface photoemission and associated satellite structures. (a) Sr $3d$ and F $1s$ emission from a thick $SrF_2$ film. (b) Ca $2p$ and F $1s$ emission from a thick $CaF_2$ film. Dashed line is predicted extrinsic losses given by $\mathrm{Im}(1/\varepsilon)$ convolved with a 1-eV Gaussian, derived from results in Ref. 19. (c) Ca $2p$ and F $1s$ emission from 1 ML CaF/Si(111) plus $\lesssim\frac{1}{4}$ layer $CaF_2$. Ca $2p$ peak is fitted to a main interface peak ($I$), an interface satellite ($I^*$) and a bulk component ($B$), as described in the text. Expanded bulk Sr $3d$ (Ca $2p$) curve has had $3d_{3/2}$ ($2p_{1/2}$) component removed assuming spin orbit parameters in the text. The spectra have been shifted to align their main peaks; they were acquired with Mg $K\alpha$ radiation ($h\nu$=1253.6 eV).

to charge transfer.[16] The first model was proposed by Veal and Paulikas[13] to account for all the $3d$ transition-metal $2p$ satellites, including the Ca $2p$ satellite at ~11 eV in $CaF_2$ [see, e.g., Fig. 1(b)]. The latter two models are discussed in detail by de Boer, Haas, and Sawatsky,[15] who suggest that the excitonic process dominates for early transition metals, including Ca, and the charge-transfer model dominates for late transition-metal insulators. In this paper, we propose that the $CaF_2$/Si(111) interface bonding state between a Ca $3d/4s$ level and a Si $3p$ level leads to a charge-transfer satellite for the interface Ca $2p$ photoemission and suppresses the excitonic satellite present for bulk $CaF_2$ emission; we find that a similar effect occurs at the $SrF_2$/Si(111) interface.

## II. EXPERIMENT

$CaF_2$ and $SrF_2$ were deposited from separate graphite or boron nitride crucibles onto resistively heated, $p$-type (≈1 Ω cm), on-axis (miscut <0.25°) Si(111) wafers in an ultrahigh-vacuum chamber. Unless otherwise noted, the substrate temperatures were 650–775 °C and the incident flux was 5–50 Å/min, calibrated with a quartz crystal oscillator. We performed photoelectron spectroscopy immediately following and in the same vacuum chamber as sample growth. The effects reported in this paper were independent of the substrate temperature and flux. Our photoelectron diffraction studies have shown the interface to be a well-ordered Si-Ca-F (Ref. 3) or Si-Sr-F (Ref. 17) structure throughout this range, although the island morphology for subsequent layers depends on the flux and temperature.[3,4,12] All films in this study were grown under conditions leading to laminar growth for their thickness. The base pressure was below $10^{-10}$ torr, and the growth pressure was typically $10^{-8}$ torr, mainly consisting of $N_2$ outgassed from BN insulators in the growth cells. The substrates were prepared using either Shiraki etching and annealing, or repeated sputter/anneal cycles until the substrates exhibited sharp 7×7 low-energy electron-diffraction (LEED) patterns and no measurable oxygen XPS signal.

XPS spectra were acquired with Mg $K_\alpha$ ($h\nu$=1253.6 eV) or synchrotron radiation ($h\nu$=135 eV) at Stanford Synchrotron Radiation Laboratory (SSRL, beamline I-1). In the case of Mg radiation, x-ray satellite lines $K_\alpha$ and $K_{\alpha 3,4}$ were deconvolved from the spectra using a Fourier transform technique. The electron spectrometer used was a hemispherical analyzer (Leybold EA-11). In addition to angle-integrated XPS measurements, we employed angle-resolved x-ray photoelectron diffraction to aid in the assignment of satellite peaks. The technique exploits angular variations of photoemission intensity, which are induced by the elastic scattering of photoemitted electrons. Previously, we used XPD to show how the interface is covered (in a layer-by-layer fashion or by bulk islands) as a function of kinetic growth parameters;[3,4] in this study, we use XPD to show that a new interface satellite does not arise from bulk $CaF_2$ atoms.

Figures 1(a) and 1(b) illustrate the experimentally observed satellites for thick films of $SrF_2$ and $CaF_2$, respectively. The samples were thick enough so that Si $2p$ signals were negligible, yet thin enough to avoid charging. Figure 1(c) depicts Ca $2p$ and F $1s$ core-level XPS spectra characteristic of ≳ a single Ca-F layer. This particular sample also contained a partial layer of $CaF_2$ above the interface layer, indicated both by the slight asymmetry in the F $1s$ spectrum, which originates from the core-level shift between buried and unburied interface F atoms,[12] and by a weak shoulder (labeled $B$ in the figure) ~2.8 eV from the main Ca $2p$ peak, which originates from the core-level shift between interface and overlying Ca atoms.[6,7] In the following paragraphs, we first discuss the satellite features observed in the bulk films, and second we will discuss the changes observed for the thin film.

The principal peak in Ca $2p$ (Sr $3d$) spectra consists of a spin-orbit-split doublet with energy splitting 3.55 eV (1.8 eV) and intensity ratio near the statistical value of 0.50 (0.67); the main F $1s$ peak is a singlet. The $2p_{1/2}$ ($3d_{3/2}$) component has been removed by a Fourier transform technique in the expanded spectra. The principal bulk peaks are clearly accompanied by satellite peaks, which have been previously discussed by several authors.[13,15,18]

Figures 1(a) and 1(b) illustrate the concept of extrinsic vs

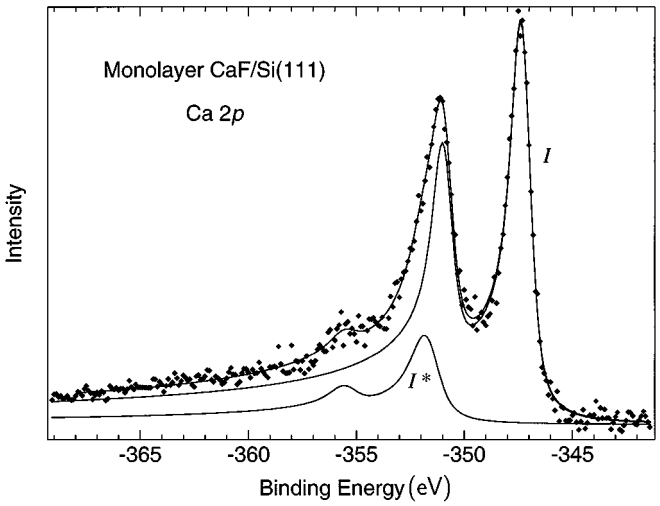


FIG. 2. Submonolayer CaF/Si(111) Ca $2p$ photoemission. The spectrum is an average of results from four films, as described in the text. Metallic line shapes were used to fit the asymmetry in the main interface Ca peak ($I$) and its satellite ($I$*).

intrinsic scattering. Extrinsic satellites are due to inelastic scattering of the electron as it traverses the film. The probability of an extrinsic energy loss $\Delta E$ is proportional to Im $[-1/\varepsilon(\Delta E)]$, and the losses should be apparent in both cation and anion emission. These losses should also be apparent in electron-energy-loss (EEL) experiments. The dielectric constant $\varepsilon(\Delta E)$ of $CaF_2$ in the range 10–35 eV has been measured by Barth *et al.* with ellipsometry[19] and inferred through Kramers-Kronig analysis from EEL measurements by Frandon, Lahaye, and Pradal;[20] the dashed line in Fig. 1(b) is the expected inelastic loss function calculated from the dielectric function in Ref. 19, convolved with a Gaussian of FWHM 1.0 eV. Comparing the photoemission satellite data to the measured $\varepsilon(\Delta E)$, it is seen that the Ca $2p$ doublets and F $1s$ peaks at 17 eV and 36 eV below the main peak arise from the dielectric losses; identification of these peaks as extrinsic satellites has also been made by direct comparison with electron energy loss spectra[20] for $CaF_2$ and $SrF_2$.[18] We note that these satellites and the associated EEL peaks are not due to ''plasmon'' excitation,[18,20,21] but rather arise from general excitations of the fluoride band structure without a sharp dip in Re($\varepsilon$). Similar loss features at ~17 and ~32 eV in the $SrF_2$ spectra are likely to arise from a similar origin, since the band structures of the two materials are quite similar[22,23] and EEL spectra of $SrF_2$ exhibit peaks at these energies.[20] The extrinsic loss peaks do not appear in the ~ single layer film [Fig. 1(c)], simply because there is almost no bulk fluoride between the interface atoms and the detector to cause an energy loss.

In addition to the extrinsic satellites, the cation and anion emission spectra exhibit intrinsic satellite peaks that are unique to the emitting ion, thus requiring the presence of a specific core hole. Several models have been proposed for the origin of these bulk satellite peaks. As discussed in the next section, we find that comparison both between the two fluorides and between bulk and interface fluoride enables selection among these models. For the bulk materials, the Ca $2p$ doublet 10.7 eV below the main peak, the Sr $3d$ peak at a loss of ~13 eV, and the three F $1s$ peaks at losses of 22–30 eV are intrinsic excitations.

The Si/fluoride interface induces a new satellite peak, which is absent from the bulk spectra. Fig. 1(c) shows results for a $CaF_2$ film $\gtrsim$1 layer thick; cation spectra from films $\leqslant$1 layer thick are presented in Figs. 2 and 4 for $CaF_2$ and $SrF_2$, respectively. At the interface, the three-peaked F $1s$ bulk satellite structure is broadened into a single peak, but the energies are comparable. As pointed out above, the extrinsic loss peaks are missing from the spectra because there is no scattering medium between the emitters and the detector. The cation intrinsic satellites characteristic of the bulk fluorides, however, are also missing from the interface emission, and are replaced by a new, low-energy satellite doublet $I$* in both $CaF_2$ and $SrF_2$.

We determined that the $I$* satellite feature in $CaF_2$/Si(111) films is directly associated with the interface Ca atom as follows. Figure 2 shows a curve fit (discussed in detail later) of a Ca $2p$ spectrum from a single CaF layer. This spectrum is an average of spectra from four different submonolayer films; no bulk peak is apparent, unlike Fig. 1(c). We verified that there were no bulklike layers using the x-ray photoelectron diffraction (XPD) technique, where the angular variation of the total interface Ca $2p$ photoemission was measured. The XPD pattern for one of the films included in the averaged spectra of Fig. 2 is shown in Fig. 3(a). Interpretation of XPD oscillations is reviewed in the literature[2] and theoretical

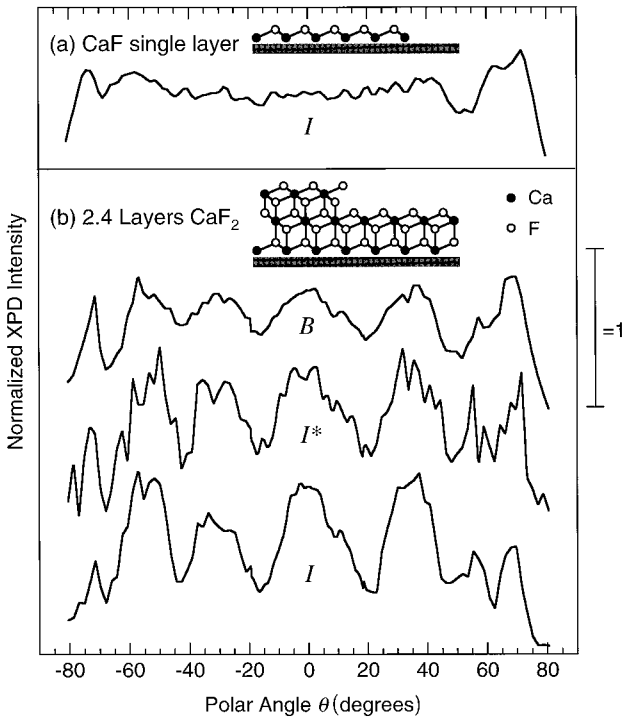


FIG. 3. Ca $2p$ x-ray photoelectron diffraction modulations. (a) Submonolayer film deposited at 650 °C (one of the four films averaged in Fig. 2). Only high-angle, intralayer Ca-F scattering is observed. (b) Component-resolved XPD modulations for a 2.4-layer film deposited at 450 °C. The ''bulk'' peak ($B$) reflects both the second and third layers; the main interface peak ($I$) and its satellite ($I$*) exhibit identical modulations, which differ both from the bulk and from the uncovered monolayer.

TABLE I. Summary of fit parameters. LW is the Lorentzian full width at half maximum (FWHM), GW is the Gaussian FWHM, $\alpha$ is the Doniach-Sunjic asymmetry. SOS is the spin orbit splitting, SOR is the spin orbit ratio, $\Delta E_f = I^*$ to $I$ energy splitting, $R = I^*$ to $I$ area ratio.

| Peak | | | LW (eV) | GW (eV) | $\alpha$ | SOS (eV) | SOR | $\Delta E_f$ (eV) | $R$ |
|---|---|---|---|---|---|---|---|---|---|
| $CaF_2$ | Ca $2p$ | $I$ | 0.56 | 0.62 | 0.24 | 3.63 | 0.57 | 4.47 | 0.32 |
| | Ca $2p$ | $I^*$ | 0.94 | 0.76 | 0.26 | 3.80 | 0.24 | | |
| $SrF_2$ | Sr $3p$ | $I$ | 1.52 | 1.26 | 0.15 | 10.3[a] | 0.55[a] | 4.82 | 0.083 |
| | Sr $3p$ | $I^*$ | 1.52[b] | 1.26[b] | 0.15[b] | 10.3[a] | 0.55[a] | | |
| | Sr $3d$ | $I$ | 0.38 | 0.91 | 0.14 | 1.75[a] | 0.67[a] | 3.83 | 0.086 |
| | Sr $3d$ | $I^*$ | 0.38[b] | 0.91[b] | 0.14[b] | 1.75[a] | 0.67[a] | | |
| $SrF_2$ | Sr $3p$ | $I$ | 2.19 | 0.97 | 0 | 10.3[a] | 0.55[a] | 4.40 | 0.15 |
| | Sr $3p$ | $I^*$ | 2.19[b] | 0.97[b] | 0 | 10.3[a] | 0.55[a] | | |
| | Sr $3d$ | $I$ | 0.42 | 1.01 | 0 | 1.75[a] | 0.67[a] | 3.60 | 0.15 |
| | Sr $3d$ | $I^*$ | 0.42[b] | 1.01[b] | 0 | 1.75[a] | 0.67[a] | | |
| | Sr $4p$ | $I$ | 0.47 | 0.70 | 0 | 1.00 | 0.50 | | 0.0 |

[a]Spin-orbit parameters derived from bulk samples.
[b]Parameters held identical for $I$ and $I^*$ peaks.

models of this CaF ML profile were recently published.[3,4] The principal result is that the Ca $2p$ intensity is uniform for emission within $|\theta| < 50°$. Such uniform emission for the high kinetic energy measured here indicates the absence of ordered bulk layers atop the interface Ca atoms, which would otherwise elastically scatter photoelectrons preferentially into principal crystal directions. Only grazing-emission scattering between Ca and F (see inset) results in XPD oscillations for $\theta \approx \pm 70°$.

Second, we established that $I^*$ is not due to any chemically distinct overlying Ca atoms and that it remains even after the interface layer is covered. From many intermediate thickness (2–8 TL) films, in which both bulklike and interface CA signals were present, the magnitude of $I^*$ was linearly correlated with the intensity of the main interface doublet; there was no apparent correlation (other than attenuation) between the intensity of $I^*$ and the amount of additional material deposited after saturation of the first layer. Spectra for 2–8 TL films may all be fitted using the monolayer Ca $2p$ spectrum in Fig. 2 as an empirical line shape for the interface contribution plus an additional doublet shifted $\sim$2.8 eV from the main interface peak for the remaining layers. This is illustrated in Fig. 1(c), where the relative heights of $I$ and $I^*$ are the same as those in Fig. 2.

Finally, we showed using chemically resolved XPD for a thicker $CaF_2$ film that the atomic site of $I^*$ is identical to $I$. Figure 3(b) shows XPD results for a $\sim$2.4 layer film grown at 450 °C, whose morphology is shown schematically in the inset. At 450 °C the interface reaction leading to CaF is not complete, and the interface layer has stoichiometry $CaF_2$.[7] Reduced diffusion on this layer leads to flatter films after two monolayers of deposition compared to higher temperatures, making it easier to distinguish bulk and interface modulation intensities.[3,4] The $I^*$ satellite exhibits the same energy and intensity in these 450 °C films as in higher-temperature films.

Detailed determination of the structure shown in the inset of Fig. 3(b) was carried out by simultaneous analysis of XPS and XPD amplitudes.[3,4] These profiles were determined by curve-fitting spectra such as in Fig. 1(c) for a spectrum acquired at each angle to three components $I$,$I^*$, and $B$. In principle, the $B$ peak can be further resolved into a contribution from middle-layer Ca atoms and surface atoms;[12] for simplicity, we have chosen here to fit $B$ to a single, large-width peak. The overall diffraction profiles of the $I$,$I^*$, and $B$ peaks are similar, indicating similar nearest-neighbor environments, although features specific to atoms buried by two additional layers of $CaF_2$,[3,4] including the dip around 60° and the shoulder at $-25°$, are present in $I$ and $I^*$ but not in $B$. Further, the oscillation amplitude of $I^*$ is identical to that of $I$, which is about twice that of $B$. The reduction of $B$ arises because this profile is the incoherent addition of two profiles: the partial third layer plus the uncovered portion of the second layer whose XPD signal resembles Fig. 3(a), and the covered portion of the second layer whose XPD signal resembles the lower profile in Fig. 3(b). The equal amplitude of $I$ and $I^*$ indicates that the Ca atoms contributing to $I^*$ and $I$ are equally buried by upper layers. Further, the $I$ and $I^*$ signals have a similar overall attenuation at large angles, which the $B$ signal does not display, which also indicates that the $I$ and $I^*$ atoms are equally buried.

Returning to Fig. 2, we show a detailed curve fit of a Ca $2p$ spectrum as two doublets, main ($I$) and satellite ($I^*$). We have used the Doniach-Sunjic line shape (convolved with a Gaussian representing the instrumental linewidth), normally used to account for the many-electron interaction between free electrons and the core hole in metal XPS spectra.[24] Table I summarizes the fit parameters. The Doniach-Sunjic lineshape was chosen because the interface Ca $2p$ peaks have a metalliclike asymmetry to them, which was not observed for any of the bulk spectra. The interface F $1s$ emission also exhibits a Doniach-Sunjic metallic line shape, although with smaller asymmetry. Valence-band photoemission, however, does not show the interface to be metallic.[25] One possible explanation is that the interface bands are only pulled below the Fermi level in the presence of the core holes. Another is that we have an additional satellite at about 1 eV that cannot

be resolved with our instrument (for example, due to crystal-field splitting, as discussed later), although this cannot account for the large inelastic tail extending ~25 eV [see Fig. 1(c)].

The fit results also show the $2p_{1/2}$ to $2p_{3/2}$ spin-orbit splitting and ratio for the satellite peak to differ from those for the main peak (~3.8 eV and ~24% vs ~3.6 eV and ~57%); both interface values differ from the bulk values (3.5 eV and 50%). Such differences in spin-orbit parameters at these high kinetic energies (~900 eV) likely arise from multiplet interactions between the $2p$ hole and the interface bonding electrons.

Finally, we note that an analogous low-energy satellite peak is absent from both bulk and interface F $1s$ spectra and from bulk Ca $2p$ spectra; the substrate Si $2p$ peak (not shown) also does not show this satellite, either with Mg $K_\alpha$ x rays ($h\nu$=1254 eV), or with soft x rays from a synchrotron ($h\nu$=135 eV). This indicates that the satellite is intrinsic to excitation of the interface Ca atom; the excitation is locally created near the core hole and cannot be excited by electrons passing through or scattering from the interface layer.

$SrF_2$ films, which have a similar interface structure to $CaF_2$ films, show similar satellite structure. Figure 4 shows F $1s$, Sr $3p$,$3d$, and $4p$ spectra for a single Sr-F layer on Si(111). The Sr $3d$ peak rides on a relatively broad plasmon loss peak of the Si $2p$ spectrum; this has been subtracted in Fig. 4. In the Sr $3p$ and Sr $3d$ spectra, a satellite double $I^*$ is present, but it is absent in the Sr $4p$ spectrum; the F $1s$ again shows no such satellite. The small shoulder on the Sr $4p$ is attributed to second-layer emission (the film from which the Sr $4p$ was acquired had a partially formed F-Sr-F triple layer atop the interface layer), although it cannot be ruled out that there is a small satellite component there as well.

Three different curve-fit procedures were considered for Sr peaks. First, we fitted the spectra to a single asymmetric doublet $I$, which assigned all the satellite intensity to an asymmetric line shape for the main peaks $I$. This procedure did not yield a satisfactory fit to any of the Sr spectra. Second, we added a satellite doublet $I^*$, which attributed some of the satellite intensity to asymmetry in $I$ and some to the distinct satellite peak $I^*$. Third, we repeated this fit with the asymmetry $\alpha$ fixed to 0. In the third fit, which is shown in Fig. 4, it was necessary to include a steplike background contribution, which we took to be proportional to the background-subtracted spectra. We then compared the reduced $\chi^2$ and quality of fit (determined by looking for systematic variations in the fit residuals). Accordingly, we determined that while the Sr $4p$ fit is acceptable with neither a satellite peak nor an asymmetric line shape (fit method 3), the Sr $3p$ and $3d$ fit best when a distinct satellite double $I^*$ is included (fit method 2 or 3). For Sr $3d$ and $3p$, the quality of fit was slightly better under methods 3 and 2, respectively. We therefore summarize both fitting methods in Table I. The main difference between the fits is a decreased amplitude (~50%) of the satellite peaks when the main peaks are assumed to have an asymmetric tail. The positions of $I^*$, however, are insensitive to the presence of the tail. For completeness, we also attempted to fit the Ca $2p$ spectrum in Fig. 2 using method 3. It was not possible, however, to fit the large inelastic tail extending out about 20 eV [see Fig. 1(c)] without adding an additional broad Gaussian. The fitted $I$-$I^*$ energy splitting using that method was within 0.1 eV of that found in Fig. 2, and the intensity ratio was dependent on the properties of the additional Gaussian.

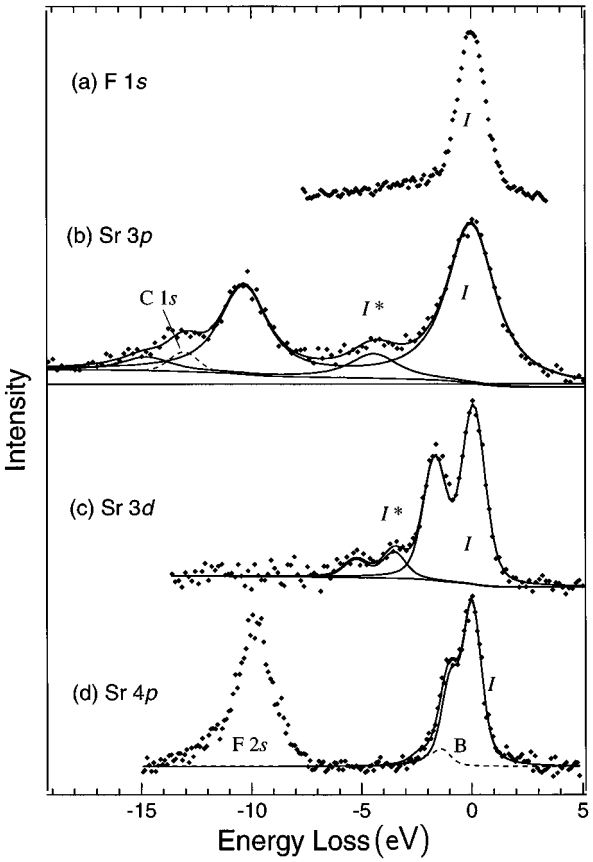


FIG. 4. Monolayer SrF/Si(111) Sr photoemission. (a) F $1s$ emission ($h\nu$=1253.6 eV); (b) Sr $3p$ emission ($h\nu$=1253.6 eV); (c) Sr $3d$ emission ($h\nu$=1253.6 eV); (d) Sr $4p$ and F $2s$ emission ($h\nu$ =135 eV). The C $1s$ (dashed) peak at −13 eV in (b) is due to C on the sample holder. In (d) the dashed Sr $4p$ peak labeled $B$, as well as the high-binding-energy shoulder on the F $2s$, are most likely due to a small amount of a second fluoride layer. The spectra have been shifted to align the main F and Sr peaks.

An important experimental result shown in Fig. 4 is that the magnitude and position of the satellite peaks depend on the particular core hole present, regardless of how the background was treated. The magnitudes range from ~10% (deeper $3p$,$3d$ core holes) to 0% (shallow $4p$ core hole), while the energy loss is larger (~4.8 vs 3.6 eV) for Sr $3p$ than for $3d$ core holes. While we did not clearly observe a satellite for Ca $3p$ emission using 135 eV photons, the overlap of the F $2s$ level with the Ca $3p$ loss region prevents a definitive assignment. It is also possible that the lower photon energy used to improve the cross section for the main-peak excitation results in a decreased probability of satellite excitation.

The observed experimental measurements of satellite energy splittings $\Delta E$ and amplitude ratios $R$ for Ca and Sr electrons are summarized in Table I. For Ca $2p$, where the spin-orbit splittings differed for the main and satellite peaks, we have used the average $\Delta E$ from the main to the satellite doublets. For Sr electrons, two different curve-fit results are shown, which differ by whether $\alpha$, the Doniach-Sunjic asym-

metry parameter, was free or held fixed at 0.0 (pure Lorentzian/Gaussian line shape). These results establish the existence of an intrinsic satellite excitation localized to the interface Ca or Sr core hole. We next consider various models to explain the observed peaks.

## III. THEORETICAL RESULTS

To understand the observed interface satellite features, we first review the bulk satellites and their literature assignments for $CaF_2$ and $SrF_2$. The bulk fluorides have a large band gap of about 12 eV, with a F $2p$-derived valence band and a Ca $4s/3d$ (Sr $5s/4d$-) derived conduction band.[22,23,26] Formation of the solid is through ionic bonds in which the two Ca $4s$ (Sr $5s$) electrons are transferred to the two F atoms in the $CaF_2$ ($SrF_2$) molecule. Both fluorides have shallow core levels 10–20 eV below the valence-band maximum, and an additional $sp$-derived conduction band predicted to be about 10 eV above the conduction-band minimum.[23,26]

### A. Anion intrinsic satellites

The F $1s$ spectra for bulk samples of both $CaF_2$ and $SrF_2$ exhibit a three-peaked intrinsic satellite structure around 25–30 eV. The monolayer F $1s$ spectrum also has structure in this energy range, but the three-peaked structure is broadened into a single peak. As we will see below, exciton formation is the most likely cause for the cation intrinsic satellites. However, this does not appear to be the case for the anion satellites. The peak energies for the bulk F $1s$ satellites are close to those of core excitons involving the shallow Ca $3p$, Sr $4p$, and F $2s$ core levels. However, this neither provides a consistent picture between the $CaF_2$ and $SrF_2$ satellites, nor explains the existence of three peaks. The strongest of the F $1s$ intrinsic loss features in $CaF_2$ is at 27.5 eV, close to the Ca $3p$ core exciton energy[19] of 27.9 eV. We measure the separation between the Ca $3p$ and F $2s$ photoemission peaks to be 3.4 eV, so that the satellite observed 30.8 eV from the main peak could be F $2s$ excitation to the same conduction-band state; there is, however, no possible core excitation within the bulk band structure for the observed satellite peak at 23.8 eV. In $SrF_2$, on the other hand, the Sr $4p$ exciton is expected at about[27] 22.5 eV (the location of the weaker F $1s$ satellite peak in $SrF_2$), and F $2s$ excitations would be $\sim$10 eV to higher binding energy (higher than either additional satellite peak).

A more likely explanation for the F $1s$ intrinsic satellites is excitation of F $2p$ valence states into higher levels in the conduction band, for example, those derived from F $3p$ and $3d$ states. Ikemoto *et al.*[18,28] suggested that F $2p-3p$ excitation is responsible for the F $1s$ satellites they observed in this energy range for LiF, NaF, KF, $MgF_2$, and $CaF_2$. Ikemoto *et al.* did not clearly observe these structures for $SrF_2$ and $BaF_2$,[18] and explained this absence by a reduced matrix element. Our observation of peaks with comparable intensity in UHV-prepared $CaF_2$ and $SrF_2$ films indicates that the low $SrF_2$ F $1s$ satellite intensity in Ref. 18 is likely due to reduced surface quality in their bulk, atmosphere-exposed samples. For $CaF_2$, measurements of Im$\varepsilon$ in the range 25–30 eV also show considerable structure, which Barth *et al.* attribute to excitations between the valence band and a set of $sp$-derived levels well above the conduction-band minimum.[19] Given the similarity of band structure for $CaF_2$ and $SrF_2$, a similar explanation is likely valid for the $SrF_2$ excitations.

The broadening of the F $1s$ satellite excitations for monolayer CaF is quite consistent with a F $2p$ excitation model. The F $2p$ and $3p$-derived states are not directly involved in interface bonding, and thus should not have large changes in energy from the bulk; however, they should have a different density of states than that characteristic of the three-dimensional band structure.

### B. Cation intrinsic satellites

We next discuss the intrinsic cation Ca $2p$ (Sr $3d$) satellites at 10.7 (13.0) eV in $CaF_2$ ($SrF_2$). The Sr $3p$ intrinsic satellite in $SrF_2$ is also at about 13 eV (not shown), but precise determination of this energy is complicated by the 10.2-eV spin-orbit splitting between the $3p_{3/2}$ and $3p_{1/2}$ components. These satellites were attributed by Ikemoto *et al.*[18] to unspecified shakeup excitations of the Ca and Sr ions. The 10.7-eV peak in $CaF_2$ was interpreted by Veal and Paulikas as due to the altered final-state screening when a ligand F $2p$ electron is not transferred to a collapsed Ca $3d$ level.[13] However, this explanation requires a drop in the $3d$ level about three times the value in the atom, which is difficult to justify.

In the exciton mode of de Boer, Haas, and Sawatsky,[15] intrinsic satellites should appear at energies close to optical excitations (peaks in Im$\varepsilon$), especially those associated with localized excitons. In the case of cation excitation, the core-hole-induced polarization of the valence-band orbitals greatly increases the overlap with the cation-derived conduction-band levels, leading to a finite probability of exciton creation. We consider this model below, taking into account the modifications of these excitations at the fluoride-silicon interface.

Comparison with the ellipsometry measurements of Barth *et al.*[19] and reflectivity measurements of Rubloff[29] establishes the bulk Ca $2p$ intrinsic loss peak (10.7 eV) to be close to the band-gap exciton energy (11.2 eV). The band-gap exciton in $SrF_2$ was observed optically at 10.6 eV;[29] while the Sr $3d$ and $3p$ intrinsic satellites are at a slightly higher energy of 13 eV. The differences between the satellite energy and the optical exciton may indicate participation of conduction-band states of $d$-like character that have their energies and charge distributions altered locally by the presence of the core hole. These states in $CaF_2$ normally lie about 1 eV above the $s$-derived conduction-band minimum[26] involved in the minimum-energy optical exciton, and are higher in $SrF_2$ than in $CaF_2$.[23] The absence of the cation-induced band-gap satellite excitation at the interface indicates that the $CaF_2$ and $SrF_2$ valence and conduction bands are strongly modified near the interface, particularly those conduction-band states localized primarily near Ca or Sr atoms. This is not surprising, since the cation sates from which the conduction-band minima are derived are involved in bonding to the Si substrate.

### C. Interface cation intrinsic satellites

At the fluoride/silicon interface, there is a missing F atom, so that an extra Ca $4s/3d$ (or Sr $5s/4d$) electron, which would have been transferred to it, is available for covalent

bonding with Si. Theoretical[30–33] and experimental[11,25,34] work on $CaF_2$ has shown that this electron and the extra Si dangling-bond orbitals form a bonding/antibonding pair of states, with a band gap of ~2.4 eV, and a possible exciton at 2.2 eV.[11] The bonding state at the $SrF_2$/Si interface has similar character to that at the $CaF_2$/Si interface.[9]

We propose that the absence of the cation excitonic loss peak at the bulk band-gap energy and its replacement by a loss peak at smaller energy is a consequence of the altered interface electronic states. We attribute the presence of $I^*$ to final-state excitations of the extra Ca valence electron; the detailed interpretation of this model depends on the extent of the electron's localization in the presence of the Ca $2p$ core hole. In the ''molecular'' limit, the altered covalent bond between the Ca $4s/3d$ and Si $3p$ valence electrons in the presence of the core hole dominates the observed satellite peak. In the ''atomic'' limit, the multiplet interaction between the Ca $3d$ electron and the core hole determine the satellite structure. We find that the molecular limit appears to explain the large satellite peaks, while the atomic interactions may account for the observed metalliclike line shapes. This is discussed further below.

Besides intrinsic excitation, it is possible that the interface satellite could arise from extrinsic losses altered by the unique dielectric function of the interface layer (although it is difficult to distinguish extrinsic from intrinsic for single-layer films). We briefly discuss this dielectric response model here. A dielectric function based on a flat (two-dimensional) joint density of states from 2.4 to 4.5 eV was found to predict the observed resonant second-harmonic generation (SHF) signals near 2.4 eV from this interface;[11] we find the same density of states also predicts a photoemission satellite peak at about 4.5 eV. This is because the SHG signal is proportional to the magnitude of the complex dielectric function $\varepsilon$, while the inelastic energy loss of electrons is proportional to Im $(1/\varepsilon)$. These functions emphasize excitations at the minimum and maximum energies in the joint density of states, respectively. While this model is consistent with both the observed SHG signal and the observed Ca $2p$ satellite in XPS, it leads to the prediction of identical satellites for both Si $2p$ and F $1s$ electrons, which we do not observe. Furthermore, it predicts identical satellites for all core excitations on the same atom, which is contrary to the differences among the various Sr levels shown in Fig. 4.

A simple molecular model, which is illustrated in Fig. 5, is sufficient to explain the observed loss peaks. Our model is based on the charge-transfer model of de Boer *et al.*,[15] who used it successfully to model satellites of late-transition-metal compounds. For clarity, we first discuss this model in terms of $CaF_2$/Si, but the interactions for $SrF_2$/Si are similar, and discussed later. The bonding state [Fig. 5(a)] is comprised of the interaction of the Si $3p$ dangling bond and the Ca $4s/3d$ singly occupied orbital. The binding energy of the Ca state relative to the Si state is given by the parameter $A$ ($A>0$ means less bound). The Hamiltonian describing the mixture of the two states is

$$H=\begin{pmatrix} A & T \\ T & 0 \end{pmatrix}, \tag{1}$$

where $T$ is the interaction energy of the two states and the basis states are the unperturbed Ca $4s/3d$ and Si $3p$ states.

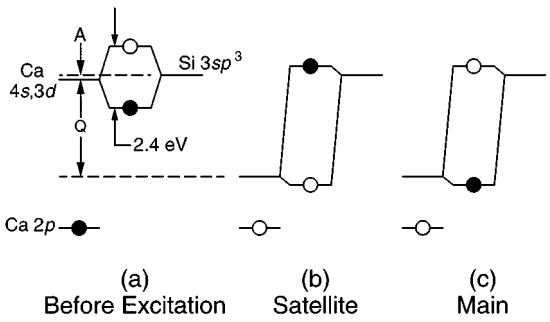


FIG. 5. Schematic of the CaF/Si interface satellite process. In the initial state, the Ca $4s/3d$ and Si dangling-bond state overlap to form a bonding/antibonding pair. After excitation of the core hole, the final state may include excitation to the antibonding state. The satellite energy difference is larger than the optical energy gap due to the collapse of the $d$ state in the presence of the core hole.

The zero of energy is defined at the Si dangling-bond level. Although we expect that $A\sim 0$ due to alignment of charge neutrality levels, we do not explicitly make this assumption. However, in any physical model $|A|$ is restricted to the range $[0, E_G]$, where $E_G$ is the interface-state band gap.

In the molecular model, the interface-state band gap $E_G$ is equated to the energy difference between the bonding and antibonding levels,

$$E_G=\sqrt{A^2+4T^2}. \tag{2}$$

We can approximate this by the band gap measured with scanning tunneling microscopy[34] and optically,[11] although this is only a rough approximation to the actual interfacial electronic states, which have reasonable dispersion (~0.5 eV across the Brillouin zone).[25] Given the band gap, we can solve for the parameter $T$ as a function of $A$ using Eq. (2).

After the creation of the Ca $2p$ core hole [Fig. 5(b)], the interaction between the Ca $3d$ electron and Ca $2p$ hole causes the Ca $3d$ electron to lower its energy by the value $Q$. In Ca, the centrifugal term $l(l+1)/r^2$ in the electronic Hamiltonian gives rise to a potential barrier for the $3d$ electron, which acts to keep the $3d$ away from the nucleus. Upon creation of the core hole, the centrifugal barrier is overcome by the attraction toward the core hole, and the $3d$ level falls in towards the nucleus.[35] A Hartree-Fock calculation by Mansfield[36] for atomic Ca gives the value $Q=3.75$ eV.

After creation of the core hole, the energy difference between Ca and Si states changes from $A$ to $A-Q$, and the interaction energy changes from $T$ to $T_f$. This alters Eqs. (1) and (2). The Si $3p$ level is assumed not to change because of the screening of the core hole by the semiconducting substrate. The new expression for the gap between bonding and anti-bonding states is

$$\Delta E_f=\sqrt{(A-Q)^2+4T_f^2}\ . \tag{3}$$

This is precisely the predicted energy loss for the satellite peak. The relative amplitude $R$ of the loss peak may be calculated in a straightforward manner from the interaction amplitudes as

$$R(A,Q,T,T_f)=\frac{|\langle f_a|i_b\rangle|^2}{|\langle f_b|i_b\rangle|^2}\ , \tag{4}$$

TABLE II. Theoretical results for the molecular model.

| | Experiment | | Band gap | Theory | |
|---|---|---|---|---|---|
| Level | $\Delta E_f$ (eV) | $R$ | $E_G$ (eV) | $Q$ (eV) | $A$ (eV) |
| Ca $2p$ | 4.5 | 0.25 | 2.4 | 3.61 | −0.20 |
| Sr $3p$ | 4.6 | 0.12 | 1.0 | 3.86 | −0.68 |
| | | | 1.5 | 3.54 | −0.91 |
| | | | 2.0 | 3.27 | −1.00 |
| | | | 2.5 | 3.05 | −0.94 |
| | | | 3.0 | 2.90 | −0.67 |
| Sr $3d$ | 3.7 | 0.12 | 1.0 | 2.99 | −0.65 |
| | | | 1.5 | 2.70 | −0.80 |
| | | | 2.0 | 2.47 | −0.76 |
| | | | 2.5 | 2.33 | −0.47 |
| | | | 3.0 | 2.29 | +0.086 |

where $|i_b\rangle$ is the wave function of the initial (bonding) state, and $|f_{a,b}\rangle$ are the possible antibonding or bonding final states.

If we assume that $T_f = T$, then the equations can be rewritten to eliminate $T$, leaving only two parameters, $Q$ and $A$. The measured quantities are the satellite splitting $\Delta E_f$ and the satellite relative magnitude $R$. We can use the above equations to find the unknowns $Q$ and $A$ given these two experimental observables. Table II shows results for $T_f = T$. For $CaF_2$ we used the interface state band gap $E_G = 2.4$ eV as measured by Heinz *et al.*[11] The solution for $Q$ at the interface, 3.6 eV, is very close to the predicted atomic value $Q = 3.75$ eV due to Mansfield.[36] The solution for $A$, −0.29 eV, is small, as expected.

For $SrF_2$ on Si, the model is similar to $CaF_2$, except that it is the $5s/4d$ state which collapses towards the core hole. Since the band gap before the core-hole creation is unknown, we have calculated the parameters $Q$ and $A$ for various values of $E_G$ in Table II. Calculations were performed for the average values of $\Delta E_f$ and $R$ from Table I.

The parameter $A$ should be independent of core hole, since it characterizes the initial state. We find that this is possible for $E_G \sim 1.0$–$1.5$ eV, $A \approx -0.6$ to $-0.9$ eV. This value of $E_G$ implies a relatively weak interaction between the initial Sr $5s/4d$ level and the Si dangling bond compared to $CaF_2$ on Si. The parameter $Q$ characterizes the final state, and may therefore be different for the different core holes. We find that $Q$ is larger (greater collapse of the $4d$ level) for the Sr $3p$ hole than for the Sr $3d$ hole. This is to be expected if the deeper Sr $3p$ hole is more localized than the Sr $3d$ hole. Since the Sr $4p$ hole is the least localized, it is consistent with this theory that there is no satellite peak which can be resolved from the main $4p$ peak.

We have also considered the possibility that $0 < T_f < T$. This is the case if the overlap of the metal $d$ level with the Si $3p$ state decreases after the $D$ wave function collapses. For $CaF_2$, we found that the values of $Q(x)$ and $A(x)$, where $0 < x = T_f/T < 1$, do not take on any unphysical values throughout the entire range of $x$ and indeed do not change drastically with $x$. For $SrF_2$, we must consider both the unknown band gap and the unknown value of $x$. We found that although $A$ varies somewhat as a function of $x$, this variation is about the same for the Sr $3d$ and Sr $4p$, regardless of the choice of band gap. Therefore whatever band gap range satisfies $A(\text{Sr } 3d) = A(\text{Sr } 3p)$ at $x = 1$ satisfies it for all values of $x$. We conclude that the molecular model gives reasonable values for the parameters $Q$ and $A$ for all values of $x = T_f/T$ for $SrF_2$.

An assumption in this section has been that the initial state has only two interacting levels, i.e., that the Ca $4s$ and $3d$ (or Sr $5s$ and $4d$) levels are nearly degenerate. This is a reasonable assumption considering theoretical calculations that show the band broadening to overlap these two levels.[23,26] However, it is far from clear whether this is reasonable in the final state, since the $3d$ level collapses inwards much more than the $4s$ level. A more refined model would consider interactions of three final states and not two. This would be invoked if the Si $3p$ level has little interaction at all (i.e., $T_f \to 0$) with the collapsed $3d$ level and if the final state consists of transitions just between $3d \to 4s$ levels. Were this the case, however, there would be very little difference in the mathematics involved—we would still be considering final-state transitions from a localized $3d$ to a (fairly) delocalized orbital.

Atomic interactions may also play a role in inducing satellite photoemission peaks. It is interesting to compare the near-edge x-ray absorption fine-structure measurements (NEXAFS) data reported by Himpsel *et al.*[37] with our results. Himpsel *et al.* observed multiple peaks at the Ca $L_{\text{II,III}}$ edge; these peaks, which result from excitations from Ca $2p \to$ Ca $3d$ states, were different for the bulk and interface Ca atoms. Interface atoms in particular displayed a strong, barely resolved feature with intensity ~25% of the main absorption peaks shifted by ~1 eV to lower absorption energy. In their interpretation, the multiplets are determined primarily by the interaction of the valence electron(s) with the core hole; effects of the rest of the solid are determined by perturbing the atomic calculations with a weaker crystal-field interaction. However, in NEXAFS of interface Ca, the experimentally observed interface transition is $2p^6(3d4s)^1 \to 2p^5(3d4s)^2$, while in XPS, the transition is $2p^6(3d4s)^1 \to 2p^5(3d4s)^1$, leading to a completely different final state. Therefore, the strong satellite that they observed should not necessarily be present in our XPS data. It

is possible, however, that the asymmetry observed in the interface cation peaks is due to these crystal field effects acting on the initial state. Furthermore, the satellite we observe at 4.5 eV should not necessarily be reflected in NEXAFS data because of the different cross sections for creating an excitation by a 900 eV electron ($\lambda \approx 0.4$ Å) vs a soft x-ray photon ($\lambda \approx 35$ Å). As mentioned earlier, the involvement of atomic multiplet interactions is evident in the Ca $2p$ emission by the altered spin-orbit splittings and ratios for interface excitation.

## IV. SUMMARY AND CONCLUSIONS

We presented experimental data supporting the existence of intrinsic satellite peaks at $CaF_2$/Si(111) and $SrF_2$/Si(111) interfaces that differ from those in the bulk fluorides. We showed that the chemically resolved x-ray photoelectron diffraction technique can be used to identify the atomic sites of satellite peaks in addition to core-level shifted peaks. The alteration of the bulk satellite peaks by interface bonding supports specific previous models for these excitations. The fluorine satellites are attributed to excitations from F $2p$-derived valence bands to higher F-derived conduction bands, which are less sharply defined at the interface than in the bulk. The cation satellites in the bulk are attributed to band-to-band transitions induced by F $2p$ polarization in the presence of the core hole. Comparison to the optical excitation energies for both $CaF_2$ and $SrF_2$ indicates that *d* states above the *s*-derived conduction-band minimum are likely involved, since the $SrF_2$ satellite energy is larger than the optical energy gap.

Several models were considered to explain the new interface satellite peaks associated with cation excitation. Key features to be explained are the reduced energy and increased strength relative to the bulk satellites, and the different energies and strengths for excitation of different core holes. The dielectric response model explains the interface Ca $2p$ line shape, but fails to account for the different splittings observed among the Sr core levels. Furthermore, the model predicts that Si core levels should have the same satellite feature, since these electrons necessarily pass through the same interface layer with similar (1150 vs 900 eV) kinetic energy. Crystal-field and multiplet interactions are likely contributing to small shifts and broadening in the line shape, but are not large enough to account for the main interface satellite. We successfully accounted for the key features of these satellites by considering the molecular interaction between interface Ca or Sr orbitals and the Si dangling-bond orbitals in the presence of a core hole. The difference between the optical gap and the satellite loss energy is attributed to the collapse of the *d*-derived component of the interface bond during core-hole excitation. In bulk transition metals, this charge-transfer satellite is predicted to occur for the late-transition metals, while the band-gap exciton model was used for early transition metals.[15] The increased covalency of the interface cation-silicon bond relative to the bulk cation-fluorine bond may account for this difference within a single metal species.

## ACKNOWLEDGMENTS

We are grateful for useful theoretical discussions with Dr. M. Hybertsen about the charge-transfer model. We also acknowledge experimental assistance from and useful discussions with M. Leskovar and U. Hessinger. E.R. and J.D.D. were resident at the University of Washington during part of this work. This research was supported by the Department of Energy under Contract No. DE-AC03-76SF00098 and DE-FG06-94ER45516. Some of the data were acquired at SSRL, which is supported by the DOE.

*Correspondence address: Center for Advanced Materials, MS 2-400, Lawrence Berkeley National Laboratory, Berkeley, CA 94720.

[1] W. F. Egelhoff, Jr., Crit. Rev. Solid State Mater. Sci. **16**, 213 (1990).
[2] S. A. Chambers, Adv. Phys. **40**, 357 (1991).
[3] J. D. Denlinger, E. Rotenberg, U. Hessinger, M. Leskovar, and M. A. Olmstead, Appl. Phys. Lett. **62**, 2057 (1993).
[4] J. D. Denlinger, E. Rotenberg, U. Hessinger, M. Leskovar, and M. A. Olmstead, Phys. Rev. B **51**, 5352 (1995).
[5] S.-P. Jeng, R. J. Lad, and V. E. Henrich, Phys. Rev. B **43**, 11 971 (1991).
[6] D. Rieger, F. J. Himpsel, U. O. Karlsson, F. R. McFeely, J. F. Morar, and J. A. Yarmoff, Phys. Rev. B **34**, 7295 (1986).
[7] M. A. Olmstead, R. I. G. Uhrberg, R. D. Bringans, and R. Z. Bachrach, Phys. Rev. B **35**, 7526 (1987); J. Vac. Sci. Technol. B **4**, 1123 (1986).
[8] R. M. Tromp and M. C. Reuter, Phys. Rev. Lett. **61**, 1756 (1988).
[9] M. A. Olmstead and R. D. Bringans, Phys. Rev. B **41**, 8420 (1990).
[10] F. J. Himpsel, U. O. Karlsson, J. F. Morar, D. Rieger, and J. A. Yarmoff, Phys. Rev. Lett. **56**, 1497 (1986).
[11] T. F. Heinz, F. J. Himpsel, E. Palange, and E. Burstein, Phys. Rev. Lett. **63**, 644 (1989).
[12] E. Rotenberg, J. D. Denlinger, M. Leskovar, U. Hessinger, and M. A. Olmstead, Phys. Rev. B **50**, 11 052 (1994).
[13] B. W. Veal and A. P. Paulikas, Phys. Rev. B **31**, 5399 (1985).
[14] I. Ikemoto, K. Ishii, H. Kuroda, and J. M. Thomas, Chem. Phys. Lett. **28**, 55 (1974).
[15] D. K. G. de Boer, C. Haas, and G. A. Sawatsky, Phys. Rev. B **29**, 4401 (1984).
[16] B. Wallbank, I. G. Main, and C. E. Johnson, J. Electron. Spectrosc. Relat. Phenom. **5**, 259 (1974).
[17] J. D. Denlinger, Ph.D. thesis, University of California at Berkeley, 1993.
[18] I. Ikemoto, K. Ishii, S. Kinoshita, and H. Kuroda, J. Electron. Spectros. Relat. Phenom. **11**, 251 (1977).
[19] J. Barth, R. L. Johnson, M. Cardona, D. Fuchs, and A. M. Bradshaw, Phys. Rev. B **41**, 3291 (1990).
[20] J. Frandon, G. Lahaye, and F. Pradal, Phys. Status Solidi B **53**, 565 (1972).
[21] K. Saiki, T. Tokoro, and A. Koma, Jpn. J. Appl. Phys. **26**, L974 (1987).
[22] R. A. Evarestov, I. V. Murin, and A. V. Petrov. J. Phys. Condens. Matter **1**, 6603 (1989).
[23] J. Kudrnovsky, N. E. Christensen, and J. Masek, Phys. Rev. B **43**, 12 597 (1991).
[24] S. Doniach and M. Sunjic, J. Phys. C **3**, 285 (1970).

[25] A. B. McLean and F. J. Himpsel, Phys. Rev. B **39**, 1457 (1989).
[26] R. A. Heaton and C. C. Lin, Phys. Rev. B **22**, 3629 (1988).
[27] This is obtained by adding the energy difference between Sr $3p$ and F $2p$, observed with photoemission (Ref. 9) to the 10.6-eV band-gap exciton (Ref. 29).
[28] I. Ikemoto, K. Ishii, S. Kinoshita, T. Fujikawa, and H. Kuroda, Chem. Phys. Lett. **38**, 467 (1976).
[29] G. W. Rubloff, Phys. Rev. B **5**, 662 (1972).
[30] K. Nath and A. B. Anderson, Phys. Rev. B **38**, 8264 (1988).
[31] H. Fujitani and S. Asano, Phys. Rev. B **40**, 8357 (1989).
[32] M. R. Salehpour, S. Satpathy, and G. P. Das, Phys. Rev. B **44**, 8880 (1991).
[33] S. Ossicini, C. Arcangeli, and O. Bisi, Phys. Rev. B **43**, 9823 (1991).
[34] P. Avouris and R. Wolkow, Appl. Phys. Lett. **55**, 1074 (1989).
[35] A. R. P. Rau and U. Fano, Phys. Rev. **168**, 7 (1968).
[36] M. W. D. Mansfield, Proc. R. Soc. London A **348**, 143 (1976).
[37] F. J. Himpsel, U. O. Karlsson, A. B. McLean, L. J. Terminello, F. M. F. de Groot, M. Abbate, J. C. Fuggle, J. A. Yarmoff, B. T. Thole, and G. A. Sawatsky, Phys. Rev. B **43**, 6899 (1991).